

Washington University in St. Louis

Washington University Open Scholarship

McKelvey School of Engineering Theses & Dissertations

McKelvey School of Engineering

Spring 5-21-2021

Injectable CT/MRI Contrast Agent for Gastrointestinal Tumor Tracking

luna zhang

Washington University in St. Louis

Follow this and additional works at: https://openscholarship.wustl.edu/eng_etds



Part of the [Bioimaging and Biomedical Optics Commons](#), and the [Biomaterials Commons](#)

Recommended Citation

zhang, luna, "Injectable CT/MRI Contrast Agent for Gastrointestinal Tumor Tracking" (2021). *McKelvey School of Engineering Theses & Dissertations*. 576.

https://openscholarship.wustl.edu/eng_etds/576

This Thesis is brought to you for free and open access by the McKelvey School of Engineering at Washington University Open Scholarship. It has been accepted for inclusion in McKelvey School of Engineering Theses & Dissertations by an authorized administrator of Washington University Open Scholarship. For more information, please contact digital@wumail.wustl.edu.

Washington University in St. Louis
McKelvey School of Engineering
Department of Biomedical Engineering

Thesis Examination Committee:

Abdel Kareem Azab, Ph.D., Chair

Hyun Kim, M.D.

Dinesh Thotala, Ph.D.

Injectable CT/MRI Contrast Agent for Gastrointestinal Tumor Tracking

By

Luna Zhang

A thesis presented to the McKelvey School of Engineering of Washington University in St.
Louis in partial fulfillment of the requirements for the degree of Master of Science.

May 2021

St. Louis, Missouri

© 2021 Luna Zhang

Dedication

Dedicated to my family and friends for their support and encouragement.

Acknowledgements

I gratefully acknowledge my thesis mentor Dr. Kareem Azab for his mentorship and guidance, for inspirational meetings, and for support with data analysis. In addition, I would like to thank Jennifer Sun for scientific discussions, reviewing this thesis, and providing valuable edits. I would also like to thank Dr. Barbara Muz for advices and encouragements, and the entire Azab Team for friendship and support.

In addition, I acknowledge Dr. Hyun Kim for project mentorship and medical insights; Dr. H. Michael Gach for imaging and instrument assistance. I acknowledge my Thesis Committee Dr. Abdel Kareem Azab, Dr. Hyun Kim and Dr. Dinesh Thotala for their valuable feedback and support.

This project was supported by the Department of Biomedical Engineering and Department of Radiation Oncology at Washington University in Saint Louis.

Luna Zhang

Washington University in Saint Louis

April 2021

Table of Contents

List of Figures	iii
Abstract	iv
Chapter 1: Introduction	1
Gastrointestinal (GI) cancer	1
Radiation therapy	2
Imaging of GI cancer	3
Magnetic resonance imaging (MRI)	3
Computed tomography (CT).....	4
Limitations for GI cancer imaging.....	5
Chapter 2: Rationale and Hypothesis.....	7
Rationale	7
Non-invasive assessment by CT & MRI	7
Choosing a contrast agent.....	7
Choosing a drug delivery system.....	8
Hypothesis.....	9
Chapter 3: Materials and Methods.....	10
Materials	10
Chitosan-based contrast agent delivery system	10
Solution preparation and cross-linked Iron-Chitosan hydrogel formation	10
Highly cross-linked Iron-Chitosan particles preparation and loading	11
PNIPAM-based contrast agent delivery system	11
Polymer solution preparation and hydrogel formation	11

CT contrast agent loading	12
MRI contrast agent loading.....	12
<i>Ex vivo</i> CT and MRI imaging	13
Chapter 4: Results	14
Chitosan-based contrast agent delivery system	14
PNIPAM-based contrast agent delivery system	16
Transparent polymer solution and opaque hydrogel.....	16
<i>Ex vivo</i> CT imaging test.....	17
<i>Ex vivo</i> MRI imaging test	18
Chapter 5: Discussion & Future Directions	22
Chapter 6: Conclusions	26
References.....	27

List of Figures

Figure 1. CT images of Iron-Chitosan hydrogel cross-linked at low density.....	15
Figure 2. CT images of highly cross-linked iron-chitosan/Matrigel system with different dose of iron NPs.....	15
Figure 3. Photographs of PNIPAM/PBS polymer solution.....	17
Figure 4. CT images of FeSO₄/PNIPAM system.....	17
Figure 5. CT images of Iron NPs/PNIPAM system.	18
Figure 6. MRI images of Iron NPs/PNIPAM system.....	19
Figure 7. MRI images of Lipid/PNIPAM system.....	20
Figure 8. MRI images of Gd₂(SO₄)₃/PNIPAM system.....	21

Abstract

Injectable CT/MRI Contrast Agent for Gastrointestinal Tumor Tracking

By

Luna Zhang

Master of Science in Biomedical Engineering

Washington University in St. Louis, 2021

Research Advisor: Associate Professor Abdel Kareem Azab

Gastrointestinal cancers remain to be of the most common and deadly cancers worldwide. Early detection and treatments are crucial for reducing mortality and improving patient outcome. Radiation therapy is a non-invasive localized tumor treatment method, and utilizes radiation to kill the cancerous cells and shrink tumors at specific sites. Precise localization at the target tumor site is therefore important before radiation therapy, especially for gastrointestinal tumor sites located in the moving bowel. Currently, invasive endoscopies along with ink tattoos are used for identifying tumor location, which often require sedation and bring much discomfort. Imaging tests, including CT and MRI, play an important role in cancer assessments due to its non-invasive ability for tumor tracking, and is often used in parallel to assists tumor localization and tracking before onset of radiation therapy.

In our study, we aimed to develop an imaging contrast agent that can be injected near the tumor site and be identified under MRI/CT imaging for non-invasive tumor localization and tracking. For the delivery system, we chose the theroresponsive polymer PNIPAM, which underdoes phase transition and crosslinks at body temperature after injection. Next, we loaded iron nanoparticles as CT contrast agent into the PNIPAM delivery system, and together they

confirmed to be effective in CT visualized tumor tracking. Lastly, we continue to investigate ways to modify classic MRI contrasts into our PNIPAM delivery system for MRI visualized tumor tracking. Together, we have designed a novel polymer-based contrast agent delivery system that has the potential to change the clinical standard and be widely beneficial by providing long-term, reliable, and non-invasive GI tumor tracking. Further studies are warranted to evaluate functional and safety profiles in mice and in patients for translation to the clinic.

Chapter 1: Introduction

Gastrointestinal (GI) cancer

Cancers in digestive tract organs such as the stomach, large and small intestine, pancreas, colon, liver, rectum, anus, and biliary system are generally designated as GI cancer [1]. While GI cancer incidence rates slightly declined in the US for the past decades, it remains to be one of the most common and fatal malignancies worldwide [2]. Currently, GI cancers collectively account for 26% of total cancer incidence and 35% of the cancer-related deaths in the world [3]. In 2018, 4.8 million new cases of GI cancers and 3.4 million related deaths were estimated worldwide [4].

GI cancers occur anywhere in the GI tract and the most common organ is stomach (60%-70%). Small intestine is the less common, ranging from 20%-30%, and the rest are found in the esophagus, large intestine, rectum, and anus [5]. In general, the symptoms of GI cancers depend on the type of cancers and occur after the tumor has become more advanced. For example, patients suffering from esophageal cancer have difficulties to swallow, while others with gastric cancer have ulcer-like symptoms [6]. Colorectal cancer can lead to changes in bowel function, lumps in the abdomen, weight loss for no reason or bleeding [7].

Since there is no obvious symptom in the early stage of GI cancer, early detection and diagnosis is important and necessary to improve the success of treatments and therefore reduce the cancer-related deaths. In the clinic, several procedures are used for GI cancer diagnosis and follow-up surveillance, which include blood tests to measure the changes in cancer markers, endoscopy to determine GI lesions and polyps, imaging study for abnormal tissue presented in the GI system, and biopsy to determine the presence of cancer cells in abnormal tissue samples.

Currently, surgery is the most common treatment for GI cancer, which involves complete removal of the tumor, along with surrounding tissue. However, such treatment could only be used for accessible and local tumors. Thus, other GI tumors which are difficult to be removed or its removal would significantly affect gastrointestinal function, will be treated by using chemotherapy, immunotherapy, targeted therapy, or radiation therapy. These advancements have reduced the number of related deaths and favorably impacted patients' prognosis and survival.

Radiation therapy

Over the past few decades, radiology techniques have played an important role in advancing cancer therapy in the clinic; radiation therapy is closely combined with surgery, chemotherapy, targeted therapy, and immunotherapy. Radiation therapy (also called radiotherapy) is a cancer treatment that uses radiation to kill cancer cells and shrink tumors. Patients with GI cancer generally radiated 5-6 weeks and can be done either before or after surgery [8]. The length of time depends on the type of GI cancers and the dose of radiation. Different from radiation used in imaging assessment, the dosage of radiation for cancer treatment is very high.

Compared to other cancer treatments such as chemotherapy, targeted therapy, and immunotherapy, radiation therapy is a highly localized cancer treatment that delivers dosages to a specific site, significantly reducing side effects while improving treatment accuracy and efficiency. One of the most crucial requirements prior to radiation therapy is the precise localization of the tumor sites, especially for some mobile tumors such as GI cancer [9]. Current localization method during follow-up treatments relies on ink tattoo injected at the tumor sites by

endoscopy. Such method is challenged by poor lighting condition, accuracy, the need for sedation, as well as repeated invasive treatments. Therefore, development of a non-invasive tumor tracking technique is direly needed to assist in locating mobile GI tumors before or during radiotherapy.

To this end, imaging techniques have emerged as the most popular techniques due to their non-invasiveness and the ability to show tumor lesions without lighting challenges. Methods such as magnetic resonance imaging (MRI), X-ray, ultrasound, computed tomography (CT), and positron emission tomography (PET), are leading to technological advances that allow non-invasive cancer assessment before or after cancer treatments.

Imaging of GI cancer

Magnetic resonance imaging (MRI)

Radiological tracking of GI system was first performed by fluoroscopy, but such examination was replaced by endoscopy and axial imaging techniques, including CT and MRI over the past 40 years [10]. MRI is a common medical imaging technique used by radiologists, with advantages such as multiplanar imaging capability, high imaging speed, good spatial resolution and high inherent soft tissue contrast [11]. Currently, MRI has been widely used in medical diagnosis and over 25,000 scanners are estimated to be used in worldwide [12].

MRI radiography provides non-invasive assessment of GI lesions and plays a significant role in detecting known or suspected malignancy to reduce the risk of cancer [13], [14]. The T1 and T2 weighting are described as MRI sequences, resulting in a particular image appearance. In the GI system, T1-weighted signals from water-like contents, such as in edema, tumor,

infarction, inflammation, infection, hyperacute or chronic hemorrhage, are shown as lower/dark MRI signals; the others, such as fat or MRI contrast agent, shorten the T1-weighted signals and show higher/bright signals under MRI [15], [16]. On the other hand, T2-weighted signals from water-like contents are higher/bright, while fat and MRI contrast agents show low/dark signals [15].

Each tissue has its specific T1- and T2- weighted signals, but different from imaging anatomical structures or blood flow, contrast agent is still required for GI tracking. The requirements for GI contrast agents include safety, insoluble, homogeneous distribution with reliable bowel marking, without peristalsis stimulation or artifacts and effective in all sequences [17], [18], [19]. The most widely used contrast agent under MRI are chelates of gadolinium-based molecules. In addition, oil emulsion, such as nutritional support formulas and baby formulas, also played an important role in GI tumor sites detection under MRI due to its low cost and widespread availability [20], [21]. Recently, iron also has been reported as an MRI contrast agent and its ability to lengthen T1 and shorten T2 has been confirmed [22].

Computed tomography (CT)

CT was first developed by Godfrey Hounsfield and Allan McLeod Cormack in the 1960s and early 1970s and became one of the most widely used imaging techniques in the clinic [23]. Currently, about 70 million patients, including about 65 million adult and 5 million children are receiving CT scans per year, and the numbers will continue to increase in the next decade [24].

CT has high accuracy and speed for the non-invasive surveillance of patients with acute abdominal complaints, known or suspected malignancy, abdominal and pelvic trauma, and inflammatory conditions [25]. Once the GI lesions or tumor sites are detected, significant

radiologic properties including the location, size, and length of involvement of the tumor sites will be analyzed using conventional radiology criteria [26]. Some additional important features, such as exophytic component, lymphadenopathy, distal metastases, adjacent mesenteric inflammatory response, phlegmon, or abscess play an important role in the differential diagnosis [26].

The strong contrast between air, soft tissue, and bone under CT facilitated the wide use of this technique in bone and lung imaging [27]. However, contrast agents are still significant for digestive tract imaging to visualize and differentiate the loops of the bowel from a pathology [28]. In general, most of the CT contrast agents are classified as positive contrasts and show bright signals under imaging. Iodine-based molecules and barium sulfate suspensions are approved by FDA for GI tumor tracking [27]. In addition, Iron nanoparticles (NPs) also emerged as a CT contrast agent for GI tumor tracking due to its safety and efficiency [29].

Limitations for GI cancer imaging

MRI and CT are important instruments for the identification of GI lesions and play a crucial role in cancer diagnosis and surveillance. However, such assessments still exhibit shortcomings specific to mobility of GI tumors. During radiation therapy, repeated imaging sessions are needed due to the loss of precise localization after the previous diagnosis. Additionally, during short-term and long-term follow-up surveillance, identification of the precise segment that was removed surgically is also critical.

The movement and the soft texture of GI system is especially difficult to be localized and identified. Therefore, accurate localization of the tumor sites remains one of the most important

tasks prior to imaging study. The major goal of MRI and CT testing for GI tumor tracking is now focused on improving the identification ability of the specific tumor sites.

In this study, we aim to design a contrast agent system that could act as a label of the specific tumor sites and could be imaged by MRI and/or CT during the subsequent assessments or following treatments.

Chapter 2: Rationale and Hypothesis

Rationale

Non-invasive assessment by CT & MRI

Previously, many tumor specific localization methods have emerged, including endoscopic tattooing, intraoperative endoscopy, intraoperative laparoscopic ultrasonography, and intraoperative fluoroscopy [30], [31], [32], [33], [34] Alginate, as a natural polymer obtained from the cell wa. However, such methods require repetition before every radiation treatment, which are time consuming and sometimes painful. On the contrary, imaging tests, including CT and MRI, provide opportunities for safer and non-invasive assessment. This gives us an opportunity to design an imaging contrast agent that can be injected near tumor lesions or treatment sites, which can be tracked from outside of human body without any invasive procedures. The contrast agents can specifically be located at the tumor sites even under the movement of the GI system, and be identified by imaging together with the tumor sites. Thus, the contrast agent acts as a label for the target tumor site and can be visualized non-invasively with imaging.

Choosing a contrast agent

Contrast agents are chemical substances used to improve the quality of MRI and CT results. Different contrast agents could show specific signals under certain imaging study. However, only a few contrast agents could show signals under both MRI and CT. Iron show strong signals under CT and emerged as an MRI contrast agent over the past few decades. Thus, in our project, we aim to use iron as an MRI/CT dual contrast agent for GI tumor tracking.

Choosing a drug delivery system

Over the past decades, biomaterial research has advanced our understanding of biomedical application through the exploitation of polymer properties. Such progressions have led to the development of polymeric drug delivery system. Polymeric drug delivery system, as a device or a cargo, facilitate the therapeutic substance to release into the body and/or adjust the rate of release. These systems are often used to improve the bioavailability and therapeutic index of the delivered drugs.

The degradation rate of the polymer material is an essential property to be studied in drug delivery engineering. In general, biodegradable and bio-absorbable polymers act as the optimal choice for many drug delivery systems to reduce cell toxicity. However, in our study, the delivery system is used as a platform to load the imaging contrast agents for an extended period of time. Therefore, the biomaterial we need in our delivery system must be stable for at least 4-6 weeks without any degradation to provide opportunity for follow up.

In addition, our delivery system is required to remain at the specific tumor sites under the movement of GI system after injection. Thus, the viscosity is another significant property for the material used in our delivery system. The high viscosity will reduce the tendency of liquid flow during GI movement, while it may lead to some difficulties for the injection. On the other hand, an injectable material with lower viscosity lacks the ability to stick in the GI wall and therefore unable to label tumor sites under movement. Therefore, choosing an appropriate material as the drug delivery system remains one of the most important tasks prior to the contrast study.

Hypothesis

In our study, we aim to develop a delivery system containing a contrast agent that can be injected near the GI tumor site into the GI wall, and can be subsequently identified through MRI/CT for non-invasive tumor assessment.

The polymeric drug delivery system could be loaded with contrast agent to form an injectable system and remain in the specific tumor sites after injection. The contrast agent loaded in the delivery system could be identified by CT/MRI study without any invasive procedures for subsequent assessments and surveillance.

Chapter 3: Materials and Methods

Materials

Unless stated otherwise, all materials used in this study were purchased from Sigma Aldrich (St. Louis, MO, USA). Chitosan (low molecular weight, 50,000-190,000 Da based-on viscosity, Sigma Product #448869), acetic acid (HAc) and glutaraldehyde (GA) solution were used for the preparation of the cross-linked chitosan hydrogels. Poly(N-isopropylacrylamide) (PNIPAM; Mn~40,000) was purchased from Sigma. Iron NPs (99.5+%, 35-45nm, metal basis) was purchased from US Research Nanomaterials INC. Corning Matrigel Basement Membrane Matrix Growth Factor Reduced (Corning, New York, NY) was prepared following manufacturer instructions.

Chitosan-based contrast agent delivery system

Solution preparation and cross-linked Iron-Chitosan hydrogel formation

Chitosan powder was dissolved in 0.1 M HAc to make a 15 mg/ml HAc-Chitosan solution and then stored at room temperature for at least 24 hours. The HAc-Chitosan solution was cooled down to 0 °C for 30 min before use. For cross-linking, GA (non-cross-linked: 0 µl/ml, or lowly cross-linked: 1 µl/ml) was added into the 0 °C HAc-Chitosan solution., vortexed immediately, heated to 60 °C in water bath for 5 min, and stored at room temperature for at least 24 hours. Then the Iron NPs were loaded at a dose of 0 mg/ml, 1 mg/ml, or 10 mg/ml, and vortexed for at least 1 min before use. The different formulations were loaded into syringes with 29-gauge needles and injected into chicken breast for *ex vivo* CT imaging.

Highly cross-linked Iron-Chitosan particles preparation and loading

Chitosan powder was dissolved in 0.1 M HAc to make a 15 mg/ml HAc-Chitosan solution and then stored at room temperature for at least 24 hours. The HAc-Chitosan solution was cooled down to 0 °C for 30 min before use. Iron NPs was added into the HAc-Chitosan solution and vortexed immediately. For a highly cross-linked hydrogel formation, GA was added into the Iron-HAc-Chitosan at a concentration of 33 µl/ml, vortexed immediately for more than 1 min, heated at 60 °C in a water bath immediately, and the gelation was observed when the transparent flowing state mixture became opaque non-flowing state. The non-flowing system was aged at room temperature overnight and then cut into pieces on culture plate and evaporated in chemical hood at room temperature for at least 24 hours. Black solid was collected after evaporation and then grounded into fine particles.

Matrigel was cooled down to 0 °C for 1 hour before use. The fine Iron-Chitosan particles were added into Matrigel and vortexed for 1 min. Then the mixture was injected into ground chicken meat for *ex vivo* CT imaging.

PNIPAM-based contrast agent delivery system

Polymer solution preparation and hydrogel formation

PNIPAM was dissolved in PBS (pH 7.4) at a concentration of 100 mg/ml, 150 mg/ml, or 200 mg/ml and stirred at 4 °C overnight. To form hydrogels, the PNIPAM solutions were heated in a 37 °C in water bath and observed every 5 seconds during gelation process. Afterwards, the hydrogels were cooled down to room temperature where the solution state was observed.

PNIPAM solutions of the above three concentrations were injected with 29-gauge needles to investigate the injectability.

CT contrast agent loading

Ferrous Sulfate

FeSO₄ powder was dissolved into PNIPAM solution at different concentration while vortexing, prior to formation of hydrogels.

Iron NPs

Iron NPs were dispersed into PNIPAM solution at different weight/volume ratios while vortexing, prior to formation of hydrogels.

MRI contrast agent loading

Iron NPs

Iron NPs were added into PNIPAM solution to make a mixture of 10 mg/ml and 20 mg/ml and then vortexed at least 1 min before use.

Lipid Solution

Tween 20, Span 80 and sesame oil were mixed at a volume ratio of 3:3:14 at room temperature and added into water to make an oil-in-water emulsion with 10% oil in the final lipid solution. Then the lipid solution was mixed with PNIPAM solution at different volume ratio.

Gadolinium Sulfate

Gd₂(SO₄)₃ powder was dissolved in water to make a saturated solution of 10 mg/ml. Then the Gd₂(SO₄)₃ solution was mixed with PNIPAM solution at different volume ratio.

***Ex vivo* CT and MRI imaging**

Ground chicken was incubated in a 24-well plate at 37 °C for at least 2 hours. 0.5cm cavities were created at the center of meat in each well.

For CT contrast, 0.1 ml of uncross-linked FeSO₄/PNIPAM or iron/PNIPAM mixtures with different ratios were added to each cavity. The meat samples were heated at 37-40 °C for 30 min and subjected to CT imaging test by Philips Brilliance Big Bore (16 slice, 85 cm gantry) and Siemens Somatom Confidence RT Pro (64 slice, 80 cm gantry).

For MRI contrast, 0.1 ml of uncross-linked Gd₂(SO₄)₃/PNIPAM mixture or lipid/PNIPAM mixture with different ratios were added to each cavity. The meat samples were heated at 37-40 °C for 30 min and subjected to MRI imaging test under Philips Ingenia 1.5 Tesla MRI simulator equipped with radiation therapy (RT) features (external laser positioning, flat tabletop, optimized pulse sequence) and Sonalleve high intensity focused ultrasound (HIFU) capabilities.

Chapter 4: Results

Chitosan-based contrast agent delivery system

We prepared two chitosan-based delivery systems loaded with iron NPs as contrast agent and tested their respective CT contrast ability. The first system is an Iron-Chitosan hydrogel cross-linked at low density and loaded with varying amounts of iron NPs. The second system is a highly cross-linked Iron-Chitosan/Matrigel system with varying amounts of iron NPs. *Ex vivo* CT imaging was performed by injecting formulations into meat samples at room temperature.

For the lower density Iron-Chitosan hydrogel, the CT signal can be detected when the iron percentage is higher than 10 mg/ml, and hydrogels with increasing GA cross-linker show better ability for delivering iron NPs under CT (**Figure 1**). However, such hydrogel seems to be challenged by leakage and cannot be used for marking specific lesion sites. On the other hand, Matrigel, as a thermoresponsive hydrogel, solidified at body temperature and is a good candidate for staying intact at a specific lesion site. However, the highly cross-linked Iron-Chitosan particles do not show any CT signals, while the iron NPs suspended in Matrigel could be detected as bright signals under CT (**Figure 2**).

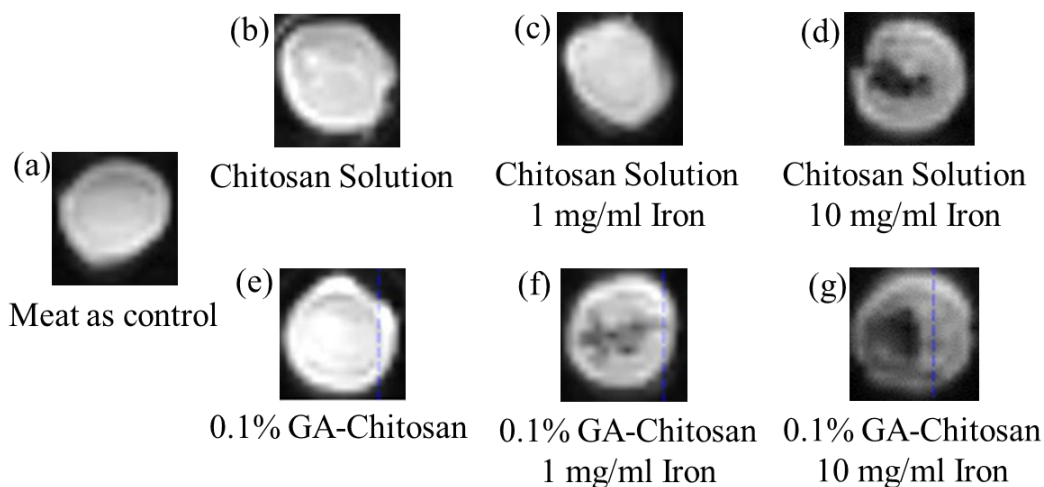


Figure 1. CT images of Iron-Chitosan hydrogel cross-linked at low density.

(a) CT image of chicken meat as control. (b, c, d) CT images of chitosan solution loaded with increasing iron concentration 0 mg/ml, 1 mg/ml, 10 mg/ml. (e, f, g) CT images of chitosan hydrogels crosslinked with 0.1 % GA loaded with increasing iron concentration 0 mg/ml, 1 mg/ml, 10 mg/ml.

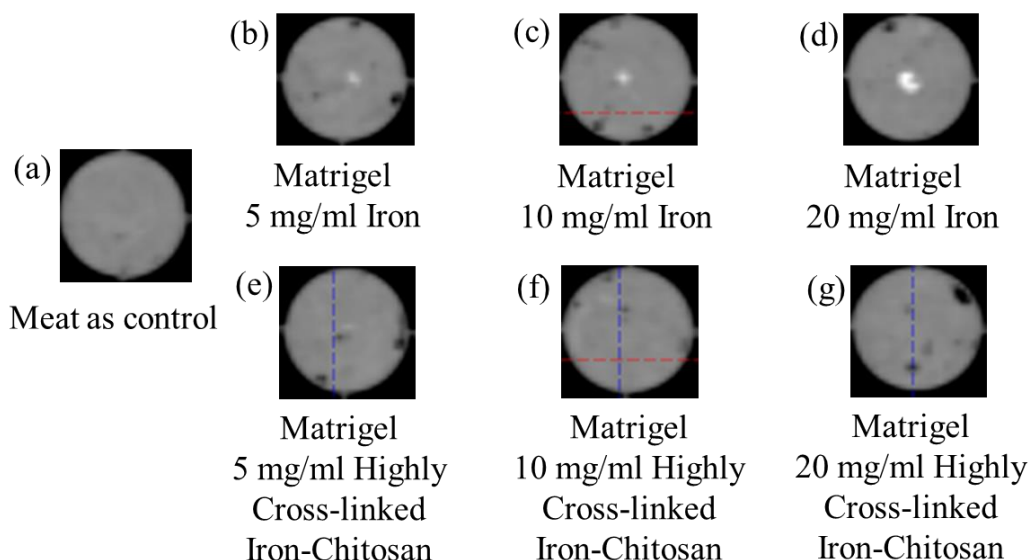


Figure 2. CT images of highly cross-linked iron-chitosan/Matrigel system with different dose of iron NPs.

(a) CT image of chicken meat as control. (b, c, d) CT images of Matrigel with increasing iron concentration 5 mg/ml, 10 mg/ml, 20 mg/ml. (e, f, g) CT images of Matrigel with increasing highly cross-linked iron-chitosan powder concentration 5 mg/ml, 10 mg/ml, 20 mg/ml.

PNIPAM-based contrast agent delivery system

Transparent polymer solution and opaque hydrogel

We aimed to find the optimal condition for PNIPAM hydrogel for our application. To this end, we dissolved varying amounts of PNIPAM and investigated its solution state and injectability. We took photographs of the solution at various temperatures and time points to document the phase transition process (**Figure 3**). The PNIPAM solution was flowing and transparent at room temperature (**Figure 3a**) but transfer into a non-flowing opaque state at 37 °C (**Figure 3b-d**) within 10 seconds due to the coil-to-globule phase transition [35]. The process transferred from transparent state to opaque state is obvious and indicates the phase transition of polymer during the following *ex vivo* imaging test. When the temperature decreases under 33 °C [36], the opaque hydrogel became a transparent solution again (**Figure 3e**). Thus, during the *ex vivo* test, temperature control after injection is significant. Although the PNIPAM solution at 200 mg/ml (**Figure 3g**) is at flowing state at room temperature, the PNIPAM solution was only injectable by 29-gauge needles at 100 mg/ml (**Figure 3a**) and 150 mg/ml (**Figure 3f**). These results demonstrated that PNIPAM could be a delivery system when kept at body temperature at 37 °C.

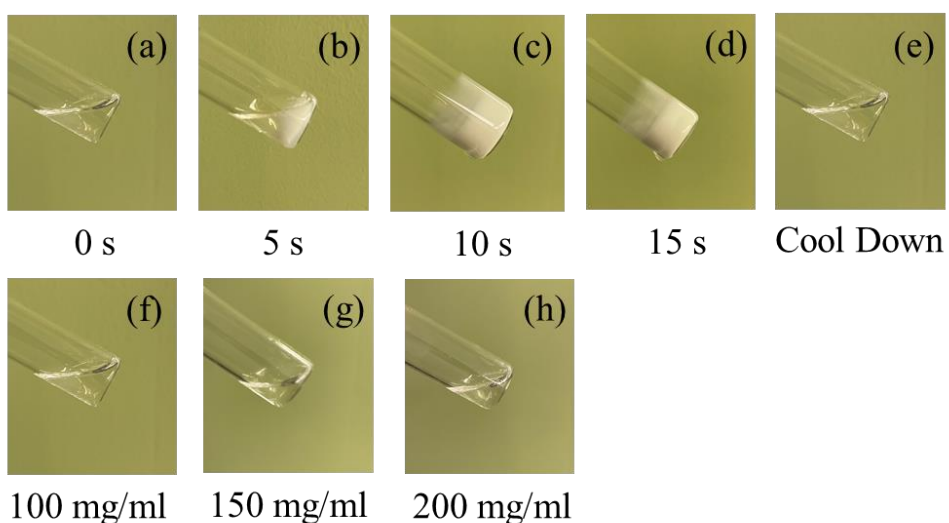


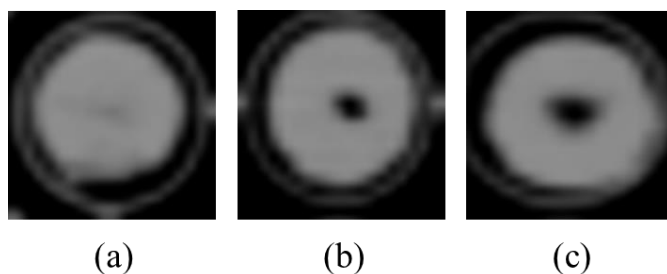
Figure 3. Photographs of PNIPAM/PBS polymer solution.

(a-e) Phase transition process for the 100 mg/ml PNIPAM/PBS polymer solution. (f) 100 mg/ml PNIPAM/PBS polymer solution at room temperature. (g) 150 mg/ml PNIPAM/PBS polymer solution at room temperature. (h) 200 mg/ml PNIPAM/PBS polymer solution at room temperature.

***Ex vivo* CT imaging test**

Then we prepared PNIPAM-based delivery system loaded with varying amounts of contrast agents such as FeSO_4 , iron NPs, lipid solution, or $\text{Gd}_2(\text{SO}_4)_3$. These formulations were injected into 37 °C meat and subjected to *ex vivo* CT and MRI imaging.

We first tested PNIPAM as a delivery system with a potential CT contrast agent FeSO_4 (**Figure 4**). The FeSO_4 /PNIPAM system did not show any bright signal compared to the meat only control. The dark signal seen in Figure 4b-c is speculated to be water contamination, or the cavity dug in the middle of the meat. These results demonstrated that Fe^{2+} does not induce CT contrast and is not suitable as contrast agent for lesion tracking under CT.

**Figure 4. CT images of FeSO_4 /PNIPAM system.**

(a) CT image of chicken meat as control group. (b) CT image of PNIPAM solution in ground chicken meat. (c) CT image of FeSO_4 /PNIPAM system in ground chicken meat.

Next, we combined iron NPs with the PNIPAM polymer delivery system at different doses of iron as CT contrast (**Figure 5**). Iron NPs at 10 mg/ml iron and 20 mg/ml both showed bright signals under CT, demonstrating that iron NPs produce signals that are strong enough to be detected, and is a promising choice for CT contrast agent for lesion tracking in our application.

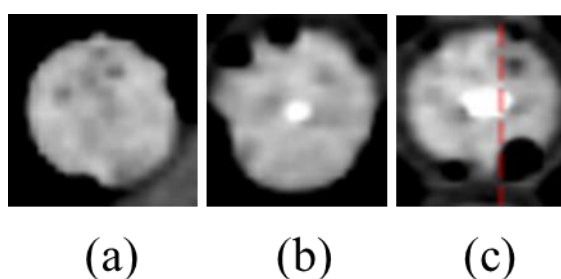


Figure 5. CT images of Iron NPs/PNIPAM system.

(a) CT image of chicken meat as control. (b) CT image of iron NPs/PNIPAM system in ground chicken meat with 10 mg/ml iron. (c) CT image of iron NPs/PNIPAM system in ground chicken meat with 20 mg/ml iron.

***Ex vivo* MRI imaging test**

Iron NPs

With a promising candidate for CT contrast, we moved onto identify an MRI contrast agent. We first tested iron NPs. MRI imaging was performed in ground chicken with the PNIPAM contrast agent delivery system kept at 37 °C. The T1-weighted signals were destroyed by iron NPs (Fig 6b-c) and there were some artifacts on T2-weighted images (Fig 6e-f). Thus, iron NPs of 10 mg/ml and 20 mg/ml are too high as a contrast agent under MRI.

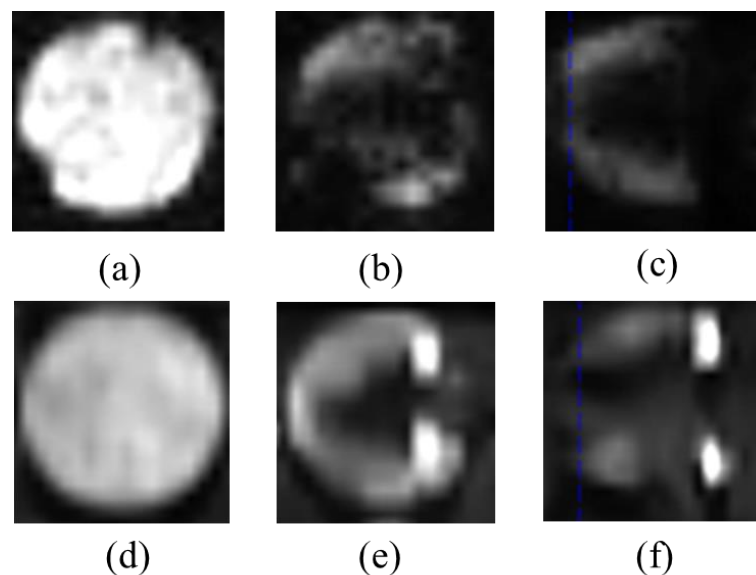


Figure 6. MRI images of Iron NPs/PNIPAM system.

(a) T1-weighted MRI image of chicken meat as control group. (b) T1-weighted MRI image of iron NPs/PNIPAM system in ground chicken meat with 10 mg/ml iron. (c) T1-weighted MRI image of iron NPs/PNIPAM system in ground chicken meat with 20 mg/ml iron. (d) T2-weighted MRI image of chicken meat as control group. (e) T2-weighted MRI image of iron NPs/PNIPAM system in ground chicken meat with 10 mg/ml iron. (f) T2-weighted MRI image of iron NPs/PNIPAM system in ground chicken meat with 20 mg/ml iron.

Lipid Solution

Next, we tested lipids as MRI contrast component for our product. Figure 7a-c shows T1-weighted MRI images of control group and lipid/polymer contrast agent system with 50% lipid. Figure 7d-f shows T2-weighted MRI images of the same samples. The dark T1 signal and bright T2 signal are obvious enough under MRI. However, lipid should show bright T1 signal and dark T2 signal based on previous studies, which is totally opposite to the results shown in Figure 7.

Therefore, the dark and bright signals are not lipid signal and we supposed it as water signal due to the water component in PNIPAM solution. However, water cannot act as a long-term marker for MRI imaging tracking. Thus, lipid/polymer is not an appropriate MRI contrast agent system for long-term tumor sites surveillance.

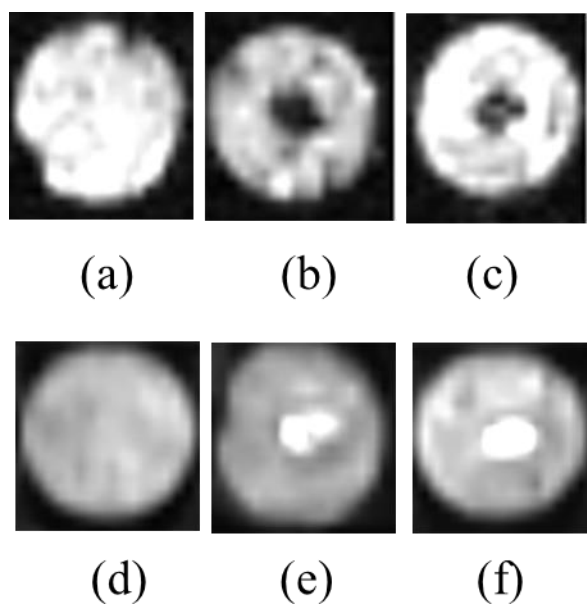


Figure 7. MRI images of Lipid/PNIPAM system.

(a) T1-weighted MRI image of chicken meat as control group. (b) T1-weighted MRI image of PNIPAM solution in ground chicken meat. (c) T1-weighted MRI image of lipid/PNIPAM (volume ratio 1:1) system in ground chicken meat. (d) T2-weighted MRI image of chicken meat as control group. (e) T2-weighted MRI image of PNIPAM solution in ground chicken meat. (f) T2-weighted MRI image of lipid/PNIPAM (volume ratio 1:1) system in ground chicken meat.

Gadolinium Sulfate

In addition, we tested $Gd_2(SO_4)_3$ /polymer contrast system as MRI contrast under the same condition. Figure 8a-b shows T1-weighted MRI images of control group and

$\text{Gd}_2(\text{SO}_4)_3$ /polymer contrast agent system. Figure 8c-d shows T2-weighted MRI images of the same samples. The images of Figure 8 do not show any obvious bright signals under T1 and dark signals under T2. Therefore, Gd^{3+} is not a perfect contrast agent under such condition for MRI tumor tracking.

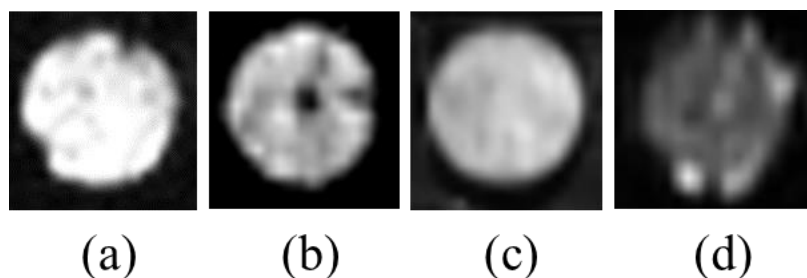


Figure 8. MRI images of $\text{Gd}_2(\text{SO}_4)_3$ /PNIPAM system.

(a) T1-weighted MRI image of chicken meat as control group. (b) T1-weighted MRI image of $\text{Gd}_2(\text{SO}_4)_3$ /PNIPAM system in ground chicken meat. (c) T2-weighted MRI image of chicken meat as control group. (d) T2-weighted MRI image of $\text{Gd}_2(\text{SO}_4)_3$ /PNIPAM system in ground chicken meat.

Chapter 5: Discussion & Future Directions

In our study, we aimed to design an injectable CT/MRI imaging contrast agent delivery system combining widely used contrast agents and polymeric biomaterial. For the choice of polymeric biomaterial, it should act as the delivery platform for contrast agents and facilitate the agents to be injected at the specific sites without leaking or degrading under GI motility.

Alginate, as a natural polymer obtained from the cell walls of brown algae, has emerged as one of the most attractive polymers used in drug delivery system. Based on our previous study, alginate could be formed into cross-linked microparticles as drug delivery system by adding dropwise to a calcium solution, which provides interaction between the divalent calcium cations and the carboxylic acid groups of two alginate chains [37]. However, such reaction is equilibrium and the microparticles will rapidly degrade into the solvent and leak its content. Thus, the imaging contrast agents cannot locate in the delivery system for a long time before the follow up surveillance.

Chitosan, as another natural polymer obtained from the hard outer skeleton of shellfish, including crab, lobster, and shrimp, plays an important role in polymeric drug delivery system. Based on our previous study, cross-linked chitosan is a perfect localized drug delivery system and the degree of cross-linking, which has some influence on drug release, depends on the concentration of cross-linkers. GA is a widely used crosslinker and the aldehyde group of GA undergoes nucleophilic attacking from the amine group of the chitosan [37]. Thus, highly cross-linked chitosan-based contrast agent delivery system had potential to be used for long-term GI tumor tracking under MRI/CT and was investigated in our study. However, the CT results of such system showed that the highest cross-linking degree that we could use for injection is not high enough for specific localization due to its gradually leaking in tissue.

Therefore, we chose a kind of thermoresponsive polymer, which exhibits phase transition triggered by body temperature after injection. Generally, polymer exhibits phase transition in response to many changes in environmental conditions, such as temperature, solvent composition, pressure, pH, ionic composition, and a small electric field [38]. Among these, temperature-induced phase transition is most common and has been thoroughly studied. Most polymers exhibit flowing state behavior under high temperature and become non-flowing state when the temperature decrease. To obtain a non-flowing polymer for our application purpose, one would need to increase the temperature before injection, which will burn the tissue and is not desirable for clinical translation.

Instead, in our project, we chose the thermoresponsive polymer PNIPAM that is opposite from the above polymers. PNIPAM exhibit a non-flowing state at high temperature and become flowing state when temperature decrease, and has a phase transition temperature of PNIPAM is 32-34 °C. The results in our study showed that at low temperature, the polymer chains fully dissolved in water due to the hydrogen bonds between the polymer and water molecules and exhibit as a coil conformation. When the temperature increased above phase transition temperature, the hydrogen bonds weakened and the coil conformation transferred to global conformation due to the dehydrated polymer chains [39]. In addition, the phase transition phenomenon could be explained by thermodynamics theory. Polymer dissolving involves mixing reaction and the binding of water molecules to the polymer chains results in a favorable enthalpy of mixing as well as unfavorable to the entropy of mixing. The entropy term is predominant at high temperature, which results in positive free energy and phase transition. Thus, the water molecules excluded from the polymer network in the process of phase separation and lead to polymer aggregation and condensation. Therefore, thermoresponsive polymer could be used as

injectable contrast agent delivery system, which can be triggered by the body temperature to go through in situ gelation for minimally invasive assessment.

After determining PNIPAM as the polymer delivering system, we moved to determine the contrast agent component. We first investigated ferrous sulfate, which should exhibit bright signals under CT. However, the small size of dissolvable ferrous ions was not large enough to be captured and retained by the PNIPAM polymer network, resulting in ferrous ions leaking out into water and cannot be a long-term contrast agent for tumor tracking under CT. To increase the size of iron, we chose iron NPs as a contrast agent under CT and found that the iron NPs loaded PNIPAM system could act as a perfect injectable CT contrast agent delivery system for GI tumor tracking.

Although we have successfully formulated a CT contrast agent for tumor tracking by non-invasive imaging study, we still aim to develop an MRI contrast system for GI tumor tracking. Lipid, as a widely used MRI contrast agent, show T1 and T2 signals under MRI, but such signals of lipid in our study were masked by water signals from PNIPAM/PBS solution. If we decrease the water content and enhance the lipid signals under MRI, the delivery system cannot be injectable under room temperature due to its high viscosity. Thus, lipid/PNIPAM cannot be a potential injectable MRI contrast system under such condition. Gadolinium is the most widely used MRI contrast agent, but the same with ferrous ions, Gd^{3+} is too small to be encapsulated by the PNIPAM polymer network. Thus, to properly deliver gadolinium with our polymer system as a potential injectable MRI contrast, further modifications of Gd^{3+} is needed to increase the molecular size of gadolinium.

For future studies, we aim to modify gadolinium to increase the molecular size by adding some chemical structure around the ions. The emergence of gadolinium chelates (GC) is leading

to technological advances of biomedical imaging for the last 25 years, boosting clinical assessments for non-invasive diagnosis [40]. The chelators provide a better thermodynamic association constant and lower dissociation kinetic rates compared to acyclic ligands [41], as well as providing chemical adjustment sites for further function. In our future study, DOTA (also known as tetraxetan) will be used as the chelator to capture the gadolinium ions and provide a chemical reaction site for structure modification. N-Hydroxysuccinimide (NHS) reactive group is introduced into DOTA and be replaced by poly(allylamine hydrochloride) to increase the size of the gadolinium-based contrast agent. The polymer chains of poly(allylamine hydrochloride) will entangled with PNIPAM and facilitate the gadolinium-based contrast agent encapsulated in the PNIPAM network for long-term imaging. Such modification will increase the size of gadolinium ions, and the same with ferrous sulfate investigated in our previous study, it will facilitate the gadolinium-based contrast agent stay in the delivery system for long time tracking.

In addition, further functional evaluation of the contrast delivery system are warranted *in vivo*. The contrast delivery system will be injected under skin of mice and the contrast efficiency will be determined, as well as the optimal contrast agent properties and dosage.

Chapter 6: Conclusions

In our study, we successfully developed an injectable CT contrast agent for GI tracking, constituting of PNIPAM solution and iron NPs. The iron NPs, acted as a contrast agent, show bright signals under CT. In parallel, the PNIPAM solution performed as an injectable material and went through phase transition triggered by the body temperature after injection. The combination of the two components potential provides opportunities for non-invasive assessment for GI tumor tracking under CT.

Our polymer-based contrast agent delivery system is a novel proposition and could has the potential to change the clinical standard and be widely beneficial by providing long-term, reliable, and non-invasive GI tumor tracking.

References

- [1] Gastrointestinal cancer. (n.d.). Retrieved April 25, 2021, from <https://www.dignityhealth.org/conditions-and-treatments/oncology/gastrointestinal-cancer>
- [2] Kamran, S., Dilling, M. K., Parker, N. A., Alderson, J., Tofteland, N. D., & Truong, Q. V. (2020). Case report: Simultaneously diagnosed gastric adenocarcinoma and pernicious anemia – a classic association. *F1000Research*, 9, 604. doi:10.12688/f1000research.24353.1
- [3] Erratum: Global cancer statistics. (2011). *CA: A Cancer Journal for Clinicians*, 61(2), 134-134. doi:10.3322/caac.20115
- [4] Arnold, M., Abnet, C. C., Neale, R. E., Vignat, J., Giovannucci, E. L., McGlynn, K. A., & Bray, F. (2020). Global burden of 5 major types of gastrointestinal cancer. *Gastroenterology*, 159(1). doi:10.1053/j.gastro.2020.02.068
- [5] www.mygenesishhealth.com. (n.d.). Radiation therapy for gastrointestinal cancers. Retrieved April 25, 2021, from <https://www.mygenesishhealth.com/treatment-options/radiation-oncology/radiation-therapy-for-gastrointestinal-cancers.html>
- [6] Gastrointestinal cancers: Symptoms, diagnosis and treatment. (2019, November 12). Retrieved April 25, 2021, from <https://www.yalemedicine.org/conditions/gastrointestinal-cancers>
- [7] Intestinal cancer | small intestine cancer. (2021, February 23). Retrieved April 25, 2021, from <https://medlineplus.gov/intestinalcancer.html>
- [8] www.mygenesishhealth.com. (n.d.). Radiation therapy for gastrointestinal cancers. Retrieved April 25, 2021, from <https://www.mygenesishhealth.com/treatment-options/radiation-oncology/radiation-therapy-for-gastrointestinal-cancers.html>
- [9] Shirato, H., Shimizu, S., Kitamura, K., Nishioka, T., Kagei, K., Hashimoto, S., . . . Miyasaka, K. (2000). Four-dimensional treatment planning and FLUOROSCOPIC real-time tumor tracking

radiotherapy for Moving tumor. *International Journal of Radiation Oncology*Biography*Physics*, 48(2), 435-442. doi:10.1016/s0360-3016(00)00625-8

[10] Mri of the gastrointestinal tract. (2010). *Medical Radiology*. doi:10.1007/978-3-540-85532-3

[11] Marciani, L. (2011). Assessment of gastrointestinal motor functions by mri: A comprehensive review. *Neurogastroenterology & Motility*, 23(5), 399-407. doi:10.1111/j.1365-2982.2011.01670.x

[12] Rinck, P. A. (2019). *Magnetic resonance in medicine a critical introduction: The basic text book of the European Magnetic Resonance Forum*. Norderstedt: Books on Demand.

[13] Fidler, J. L., Guimaraes, L., & Einstein, D. M. (2009). Mr imaging of the small bowel. *RadioGraphics*, 29(6), 1811-1825. doi:10.1148/rg.296095507

[14] Zijta, F. M., Bipat, S., & Stoker, J. (2009). Magnetic resonance (mr) colonography in the detection of colorectal lesions: A systematic review of prospective studies. *European Radiology*, 20(5), 1031-1046. doi:10.1007/s00330-009-1663-4

[15] Wayback machine. (n.d.). Retrieved April 25, 2021, from https://web.archive.org/web/20170510065614/https://www.radiology.wisc.edu/education/med_students/neuroradiology/NeuroRad/Intro/MRIintro.htm

[16] Basic proton mr imaging. (n.d.). Retrieved April 25, 2021, from <https://web.archive.org/web/20160305000107/http://www.med.harvard.edu/aanlib/basicsMR.html>

[17] Kressel, H. Y. (1991). Insights of an abdominal imager: What do we need for mri enhancement? *Magnetic Resonance in Medicine*, 22(2), 314-318. doi:10.1002/mrm.1910220232

- [18] Hahn, P. F. (1991). Advances in contrast-enhanced mr imaging. gastrointestinal contrast agents. *American Journal of Roentgenology*, 156(2), 252-254. doi:10.2214/ajr.156.2.1898795
- [19] Brown JJ. (1996) Gastrointestinal contrast agents for MR imaging. *Magnetic Resonance Imaging Clinics of North America*, 4(1):25-35.
- [20] Mirowitz, S. A., & Susman, N. (1992). Use of nutritional support formula as a gastrointestinal contrast agent for mri. *Journal of Computer Assisted Tomography*, 16(6), 908-915. doi:10.1097/00004728-199211000-00015
- [21] Balzarini, L., Aime, S., Barbero, L., Ceglia, E., Petrillo, R., Reyner, J., . . . Musumeci, R. (1992). Magnetic resonance imaging of the gastrointestinal tract: Investigation of baby milk as a low cost contrast medium. *European Journal of Radiology*, 15(2), 171-174. doi:10.1016/0720-048x(92)90148-3
- [22] Queiroz-Andrade, M., Blasbalg, R., Ortega, C. D., Rodstein, M. A., Baroni, R. H., Rocha, M. S., & Cerri, G. G. (2009). Mr imaging findings of iron overload. *RadioGraphics*, 29(6), 1575-1589. doi:10.1148/rg.296095511
- [23] Goodman, L. R. (2010). The Beatles, the Nobel prize, and CT scanning of the chest. *Radiologic Clinics of North America*, 48(1), 1-7. doi:10.1016/j.rcl.2009.09.008
- [24] Brenner, D. J. (2010). Should we be concerned about the rapid increase in ct usage? *Reviews on Environmental Health*, 25(1). doi:10.1515/reveh.2010.25.1.63
- [25] Macari, M., & Balthazar, E. J. (2001). CT of bowel Wall thickening. *American Journal of Roentgenology*, 176(5), 1105-1116. doi:10.2214/ajr.176.5.1761105
- [26] Balthazar, E. J. (1991). CT of the GASTROINTESTINAL TRACT: Principles and interpretation. *American Journal of Roentgenology*, 156(1), 23-32. doi:10.2214/ajr.156.1.1898566

- [27] Kim, J., Chhour, P., Hsu, J., Litt, H. I., Ferrari, V. A., Popovtzer, R., & Cormode, D. P. (2017). Use of Nanoparticle contrast agents for cell tracking with computed tomography. *Bioconjugate Chemistry*, 28(6), 1581-1597. doi:10.1021/acs.bioconjchem.7b00194
- [28] Gastrointestinal contrast media For CT Scan Study. (n.d.). Retrieved April 25, 2021, from <http://www.radtechonduty.com/2017/03/gastrointestinal-contrast-media.html>
- [29] Hemalatha, T., Prabu, P., Gunadharini, D. N., & Gowthaman, M. K. (2018). Fabrication and characterization of dual Acting oleyl chitosan functionalised iron Oxide/gold HYBRID nanoparticles for MRI and CT imaging. *International Journal of Biological Macromolecules*, 112, 250-257. doi:10.1016/j.ijbiomac.2018.01.159
- [30] Ohgami, M., Otani, Y., Kumai, K., Kubota, T., Kim, Y., & Kitajima, M. (1999). Curative laparoscopic surgery for Early GASTRIC Cancer: Five years experience. *World Journal of Surgery*, 23(2), 187-193. doi:10.1007/pl00013167
- [31] Park, D. J., Lee, H. -, Kim, S. G., Jung, H. C., Song, I. S., Lee, K. U., . . . Yang, H. (2005). Intraoperative gastroscopy for gastric surgery. *Surgical Endoscopy*, 19(10), 1358-1361. doi:10.1007/s00464-004-2217-0
- [32] Hyung, W. J., Lim, J. S., Cheong, J. H., Kim, J., Choi, S. H., Song, S. Y., & Noh, S. H. (2005). Intraoperative tumor localization using laparoscopic ultrasonography in laparoscopic-assisted gastrectomy. *Surgical Endoscopy*, 19(10), 1353-1357. doi:10.1007/s00464-004-8196-3
- [33] Beretvas, R., & Ponsky, J. (2001). Endoscopic marking: An adjunct to LAPAROSCOPIC gastrointestinal surgery. *Surgical Endoscopy*, 15(10), 1202-1203. doi:10.1007/s004640000304

- [34] Nagata, K., Endo, S., Tatsukawa, K., & Kudo, S. (2007). Intraoperative fluoroscopy vs. intraoperative laparoscopic ultrasonography for early colorectal cancer localization in laparoscopic surgery. *Surgical Endoscopy*, 22(2), 379-385. doi:10.1007/s00464-007-9415-5
- [35] Schild, H. (1992). Poly(n-isopropylacrylamide): Experiment, theory and application. *Progress in Polymer Science*, 17(2), 163-249. doi:10.1016/0079-6700(92)90023-r
- [36] Shi, K., Wang, Y., Qu, Y., Liao, J., Chu, B., Zhang, H., . . . Qian, Z. (2016). Synthesis, characterization and application of reversible PDLLA-PEG-PDLLA copolymer thermogels in vitro and in vivo. *Scientific Reports*, 6(1). doi:10.1038/srep19077
- [37] Puente, P. D., Fettig, N., Luderer, M. J., Jin, A., Shah, S., Muz, B., . . . Azab, A. K. (2018). Injectable hydrogels for Localized chemotherapy and radiotherapy in brain tumors. *Journal of Pharmaceutical Sciences*, 107(3), 922-933. doi:10.1016/j.xphs.2017.10.042
- [38] Amiya, T., & Tanaka, T. (1987). Phase transitions in crosslinked gels of natural polymers. *Macromolecules*, 20(5), 1162-1164. doi:10.1021/ma00171a050
- [39] Cao, M., Wang, Y., Hu, X., Gong, H., Li, R., Cox, H., . . . Lu, J. R. (2019). Reversible thermoresponsive Peptide–PNIPAM Hydrogels for controlled drug delivery. *Biomacromolecules*, 20(9), 3601-3610. doi:10.1021/acs.biomac.9b01009
- [40] Stasiuk, G. J., & Long, N. J. (2013). The ubiquitous DOTA and its derivatives: The impact of 1,4,7,10-tetraazacyclododecane-1,4,7,10-tetraacetic acid on biomedical imaging. *Chemical Communications*, 49(27), 2732. doi:10.1039/c3cc38507h
- [41] Sherry, A. D., Caravan, P., & Lenkinski, R. E. (2009). Primer on gadolinium chemistry. *Journal of Magnetic Resonance Imaging*, 30(6), 1240-1248. doi:10.1002/jmri.21966